An Electrochemical Approach of the Redox Behavior of Water Insoluble Ubiquinones or Plastoquinones Incorporated in Supported Phospholipid Layers

Damien Marchal, Wilfrid Boireau, Jean Marc Laval, Jacques Moiroux, and Christian Bourdillon
Laboratoire de Technologie Enzymatique, Unité Associée au CNRS N° 1442, Université de Technologie de Compiègne, BP 529, 60205 Compiègne Cedex, and the Laboratoire d'Electrochimie Moléculaire, Unité Associée au CNRS N° 438, Université de Paris 7-Denis Diderot, 75251 Paris Cedex 05, France

ABSTRACT Physiological mole fractions of long isoprenic chain ubiquinone (UQ_{10}) and plastoquinone (PQ_9) were incorporated inside a supported bilayer by vesicle fusion. The template of the bilayer was an especially designed microporous electrode that allows the direct electrochemistry of water insoluble molecules in a water environment. The artificial structure, made by self-assembly procedures, consisted of a bilayer laterally in contact with a built-in gold electrode at which direct electron transfers between the redox heads of the quinones molecules and the electrode can proceed. The mass balances of quinone and lipid in the structure were determined by radiolabeling and spectrophotometry. A dimyristoyl phosphatdylcholine stable surface concentration of 250 ± 50 pmol · cm^{-2}, unaffected by the presence of the quinone, was measured in the fluid monolayer. The mole fraction of quinone was between 1 and 3 mol%, remaining unchanged when going from the vesicles to the supported layers. The lipid molecules and the quinone pool were both laterally mobile, and cyclic voltammetry was used to investigate the redox properties of UQ_{10} and PQ_9 over a wide pH range. Below pH 12, the two electrons–two protons electrochemical process at the gold electrode appeared under kinetic control. Thus all thermodynamic deductions must be anchored in the observed reversibility of the quinone/hydroquinol anion transformation at pH > 13. Within the experimental uncertainty, the standard potentials and the pK_a's of the pertinent redox forms of UQ_{10} and PQ_9 were found to be essentially identical. This differs slightly from the literature in which the constants were deduced from the studies of model quinones in mixed solvents or of isoprenic quinones without a lipidic environment.

INTRODUCTION

In mitochondria and chloroplast electron transfer chains, the redox and physicochemical properties of polyisoprenic quinones are central points of interest. However, despite numerous attempts (for reviews, see Swallow, 1982; Rich, 1984; Crane and Barr, 1985; Okamura and Feher, 1992), it has not been possible to assign definitive values to the operative thermodynamic constants concerning the redox reactivity of the biological quinones incorporated in the bilayer. The reason for this lies in the amphiphilic nature of the molecules. The extreme hydrophobicity of the tail, often consisting of more than seven isoprenic groups of physiological quinones, precludes classical measurements of the extent of redox reactivity in an aqueous environment. On the other hand, the mechanisms and the thermodynamics depend on the quinone environment. Different approaches have been developed in the past to try to overcome the contradiction and to estimate the relevant thermodynamic constants. At first, the electrochemical behavior of model quinones, solubilized in water or organic solvents, was investigated. The organic solvents were aprotic (Cauquis and Marbach, 1972; Chambers, 1974; Prince et al., 1983, 1986), or were supplemented with proton donors (Marcus and Hawley, 1971; Cauquis and Marbach, 1972). The redox reactivity of physiological molecules like ubiquinone-10 (UQ_{10}) or plastoquinone-9 (PQ_9), solubilized in hydroalcoolic solutions, was also examined (Land and Swallow, 1970; Morrisson et al., 1982; Prince et al., 1983). Recently, various self-assembly methods were used to incorporate UQ_{10} at the interface between water and modified electrodes, either by means of direct adsorption at the electrode surface (Ksenzhek et al., 1982; Schrebler et al., 1990; Takehara and Ide, 1991; Gordillo and Schiffrin, 1994) or by incorporation into an alkanethiol monolayer (Takehara et al., 1991) or a phospholipid monolayer (Moncelli et al., 1996) deposited on the electrode surface.

Thus it is of significant interest to be able to characterize the electron and proton transfers involving the quinone moiety in such a way that water molecules would be available for the redox center while a lipidic environment is available for the tail.

From the mechanistic point of view, the quinone/quinol transformation is rather complex, because of the fact that the overall two hydrogen atom–two electrons transfer may proceed through several possible routes, each one being more or less favored by the nature of the environment. Theses routes can be conveniently represented in "square schemes" (Laviron, 1984; Meunier-Prest and Laviron, 1992; Chambers, 1974). If the redox transformation takes place within a structure like a lipidic bilayer, the question that arises

Received for publication 10 December 1996 and in final form 10 March 1997.

Address reprint requests to Dr. Christian Bourdillon, Laboratoire de Technologie Enzymatique, Unité Associée au CNRS N° 1442, Université de Technologie de Compiègne, BP 529, 60205 Compiègne Cedex, France. Tel.: 33-03-44234405; Fax: 33-03-44203910; E-mail: christian.bourdillon@utc.fr.

0006-3495/97/06/2679/09 $2.00

readily concerns the proton availability for the proton transfers that may accompany the electron transfers. Furthermore, the reaction pathway can also be altered significantly by the binding of the quinone to a specific site of a membrane protein. The latter aspect is beyond the scope of the present paper.

Numerous model membrane systems have been developed for studying the physicochemical behavior of molecules inside a bilayer (for a review see Gennis, 1989). These model systems can be grouped as planar bilayers, supported or not, and vesicles, unilamellar or multilamellar. Direct electrochemistry inside the hydophobic part of these structures is not an easy task, because the working electrode has to be positioned correctly, at the molecular level, in the structure. This seems impossible in the spherical geometry of vesicles, but a new technology has been developed for supported bilayers (Miller and Majda, 1986; Torchut et al., 1994). The key is a special design of a modified electrode, which is used as the template for the bilayer. One such design involves electrodes coated with microporous aluminium oxide films. The geometry of the template produces an array of cylindrical pores, which are oriented perpendicular to the electrode interface (Fig. 1 *A*). The first hydrophobic layer is obtained by self-assembly of an alkyl silane on the aluminium oxide template. The final phospholipid layer is formed by vesicle fusion on the inner surface of the hydrophobic pores (Torchut et al., 1994). This spontaneous fusion of lipidic vesicles could be very useful for introducing into the artificial bilayer any hydrophobic or amphiphilic molecule that is easy to manipulate inside vesicles. For example, methods for the incorporation of ubiquinone or plastoquinone molecules in vesicles are known, at least for low quinone/lipid ratios. Fusion of such vesicles could lead to a supported bilayer containing the hydrophobic quinones, as described in Fig. 1 *B*.

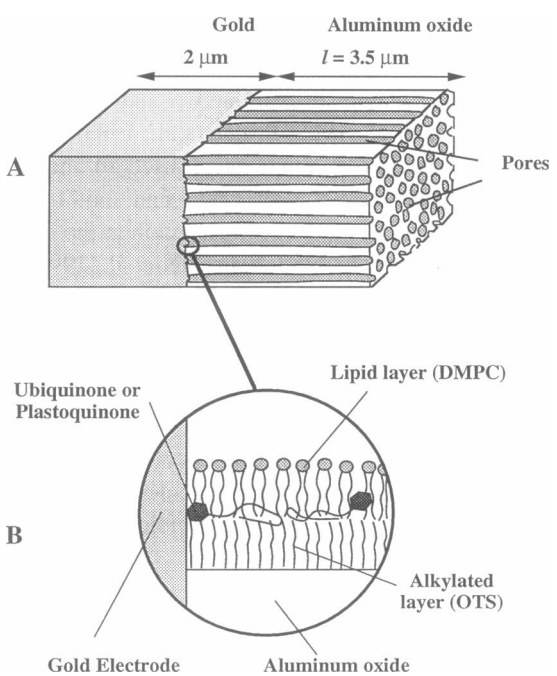

FIGURE 1 (*A*) General structure of a porous aluminium oxide film attached to a gold electrode. The average pore diameters of the film were 90 ± 10 nm. (*B*) Schematic view of the electrode/bilayer interface. The alkylated/lipid bilayer is assembled on the inner surface of the porous aluminium oxide film. The DMPC and isoprenic quinone molecules are laterally mobile along the pores.

The aim of the present work was to determine quantitatively the thermodynamics of the redox reactivity of physiological isoprenic quinones solubilized in a physicochemical environment mimicking as closely as possible the structure of a biological membrane. First of all, we had to ascertain that the fusion of phospholipid/quinone vesicles on the microporous electrode is quantitative and produces a bilayer containing isoprenic quinones at the physiological level. The resulting quinone pool was found to be quite mobile in the bilayer, and its redox state was electrochemically controlled, that is to say, oxidized or reduced directly into the structure. A careful study of the electrochemical behavior as a function of pH enabled us to discuss the mechanisms of proton and electron exchanges between the redox head of the molecule, the electrode, and the environment.

MATERIALS AND METHODS

Reagents

L-α-Dimyristoyl phosphatidylcholine (DMPC), synthetics > 99% pure, was purchased from Sigma (St. Quentin Fallavier, France). L-α-1,2-Di(1-^{14}C)palmitoyl phosphatidylcholine (^{14}C-DPPC), 50 mCi/mmol, was from Amersham (Les Ulis, France). Ubiquinone 10 (UQ_{10}), ubiquinone 2 (UQ_2), and plastoqinone 9 (PQ_9) were from Sigma. *N*-Methyl-*N'*-octadecyl-4,4'-bipyridinium dichloride ($C_{18}MV$) was synthesized according to the method of Pileni et al. (1980). Octadecyltrichlorosilane (OTS) (Aldrich, Strasbourg, France) was vacuum distilled before use. Hexadecane (Aldrich) was dried over desiccated molecular sieves. Aluminum foil, 1 mm thick (Al 99.95%), was from Merck (Darmstadt, Germany). Thick aluminium oxides (thickness 60 μm) were commercial inorganic membrane filter discs (Anodisc 47; porosity 0.1 μm) from Whatmann (Maidstone, England). Organic solvents were high-performance liquid chromatography grade. All other chemicals were reagent grade.

Preparation of the OTS-treated oxides and aluminum oxide-coated gold electrodes

Commercial thick aluminum oxide films (Anodisk 47) were first pretreated in a 0.05 M NaOH solution for 4 min and rinsed in water. After drying, the oxide films were alkylated into a freshly prepared 2% solution (v/v) of OTS in hexadecane. After a 15-min self-assembly, they were rinsed extensively with toluene and used immediately. The actual surface area of the pores was evaluated from scanning electron microphotographies at a magnification of 20,000×. The average diameter of the pores was 190 nm, and the number of pores was 1.3×10^9 pores/cm^2, given a porosity of 0.37. Taking account the thickness of the film, the actual surface area/geometrical surface area ratio was 450 ± 80.

The modified electrodes were prepared with very thin aluminium oxide films (a few microns) produced in the laboratory. The procedure was first described by Miller and Majda (1986) and modified by Parpaleix et al. (1992). Briefly, aluminum oxide films were generated by anodization of aluminum foil. The separation of the oxide film from the aluminum substrate and the removal of the barrier layer were performed according to

the method of Parpaleix et al. (1992). The average thickness of these films was 3.5 ± 0.4 μm and was routinely controlled by scanning electron microscopy. Fabrication of the gold electrodes coated with OTS-treated oxide films involved the following additional steps. Dried thin oxide films were transferred into a freshly prepared 2% solution (v/v) of OTS in hexadecane. After a 15-min self-assembly, they were carefully rinsed with toluene and transferred into a vacuum deposition apparatus (Edwards model E306A), where they were coated with ~2-μm-thick gold films (thus it is worth underlining that the gold surface is not coated with OTS, and confirmation can be found in the value of the capacitive current measured in cyclic voltammetry). Finally, the gold-coated oxide films were mounted on the tip of a glass tube (3 mm in diameter) according to the method of Miller and Majda (1986). The geometrical surface area of the electrode was 0.07 cm^2. Taking account of the oxide geometry (average diameter of the pores 90 nm, 5.1 × 10^9 pores/cm^2, porosity 0.4), the actual surface area/geometrical surface area ratio was 50 ± 8, and the internal aluminum oxide surface area and thus the bilayer surface area were 3.7 ± 0.7 cm^2.

The final quality of the microporous electrodes was routinely controlled by using the procedure described by Torchut et al. (1994). A chronocoulometric measurement was performed on each electrode after the self-assembly of a layer of $C_{18}MV$ (this loading can easily be removed by a methanol washing). All modified electrodes giving a lateral diffusion coefficient of $C_{18}MV$ smaller than 8 × 10^{-8} $cm^2 \cdot s^{-1}$ at 30°C or/and a surface concentration of $C_{18}MV$ lower than 120 $pmol \cdot cm^{-2}$ were discarded.

Supported monolayer assemblies

Phospholipid vesicles were prepared from dried lipids as follows. A known amount of DMPC (~8 mg) was resuspended from the walls of a glass tube by vigorous vortexing in 9 ml of water. This solution was sonicated to clarity, four times for 3 min each with a Branson model 250 sonicator (Danbury, CT) set at 60 W power, the temperature being maintained between 40°C and 50°C, using a cold bath in case of need. This stock solution (~1.3 × 10^{-4} M) was cleaned from titanium particles by centrifugation at 3000 × *g* and used for dilutions during the day. The mixed vesicles of DMPC and quinones were prepared at a quinone mole fraction two times the one expected in the bilayer (see Results and Discussion). DMPC and UQ_{10} (or PQ_9) at the required ratio in chloroform were evaporated together under nitrogen, resuspended, and sonicated as above.

Direct fusion of unilamellar vesicles of lipids on the inner surfaces of OTS-treated microporous aluminum oxide templates followed the procedure originally described for alkylated glass coverslips by Brian and McConnell (1984). The microporous electrodes or the thick oxides were first wetted with methanol and rinsed with water in three different baths. The wetted oxides were then transferred and incubated for 5 h in the vesicle solution (7 10^{-4} M) for adsorption and fusion at 30°C. Before use, the oxides were extensively rinsed with water for at least 30 min to remove the adsorbed vesicles.

Quinone and lipid assays

Because of the small surface area of the thin oxide films coated on electrodes, only a radioactive labeling method could be used to measured the amount of DMPC. Radioactively labeled lipid, [^{14}C]DPPC, was introduced at the 1 mol% level into the lipid solution in chloroform. The same procedures as described above were followed to prepare the supported monolayer assemblies. After extraction in methanol, the radioactivity was measured with a model LS8000 scintillation counter (Beckman, Fullerton, CA), as previously described (Torchut et al., 1994).

For thick oxide films, UQ_{10} and DMPC surface concentrations were both measured in the same experiment. Some pieces of oxide films, that is to say, the equivalent of about 1500 cm^2 of porous surface area, were first treated as above to produce the supported assembly of UQ_{10} and DMPC (labeled with 0.04 mol% with [^{14}C]DPPC) on the OTS layer. After rinsing, the oxide pieces were carefully transferred with tweezers in a centrifugation tube for extraction. Then 0.5 ml of methanol, 0.5 ml of water, and 1 ml of chloroform were successively added, with a vortexing step between additions. The chloroform phase was separated after 5 min of centrifugation at 1200 × *g*. An aliquot of 0.1 ml was diluted in 5 ml of the liquid scintillation cocktail for radioactive counting. Concurrently, the absorption spectrum of the chloroform phase was recorded (model 8452A spectrophotometer; Hewlett Packard, Waldbronn, Germany). The absorbance maximum at 275 nm was used for UQ_{10} assay (molar absorbance in chloroform 15,500 M^{-1} cm^{-1}).

The principle of measurements of the UQ_{10} mole fractions in vesicles was essentially the same as for thick oxides, i.e., 0.5 ml of the vesicles suspensions was extracted with 0.5 ml of methanol and 1 ml of chloroform. The chloroform phases were counted and spectrophotometrically assayed.

Electrochemical measurements

An anaerobic electrochemical cell was fitted with three electrodes: a working microporous oxide film electrode, a saturated KCl calomel electrode (SCE = 0.238 V versus normal hydrogen electrode at 30°C) as the reference electrode, and a platinum foil counter electrode. The last one was introduced in a solution separated from the main compartment by a glass frit.

For the measurements at different pH, the background solutions were prepared as follows. pH 4 to 7: 0.01 M citric acid/citrate buffers. pH 7 to 8: 0.01 M phosphate buffers. pH 8 to 11: 0.01 M carbonate buffers. pH 11 to 13: NaOH solutions. When necessary, the buffers were adjusted at 0.1 M ionic strength with Na_2SO_4. Gentle bubbling of argon reduced the partial pressure of oxygen in the main compartment to a low level. The temperature was controlled at 30°C by water circulation in the outer jacket of the cell.

A PAR model 273 potentiostat controlled by a PC computer and model 270 software package (EG&G Princeton Applied Research, Princeton, NJ) was used for excitation and measurement in cyclic voltammetric and chronocoulometric experiments.

RESULTS AND DISCUSSION

The chain-melting phase transition temperature (T_m = 23.5°C) of DMPC being close to 25°C, all experiments were carried out at 30°C, i.e., well above T_m.

The bilayer structure

The vesicle fusion mechanism was used to incorporate the UQ_{10} or PQ_9 water-insoluble molecules into the supported bilayer. The alkylated microporous electrodes were thus incubated in either a pure DMPC vesicle solution or a mixed DMPC/quinone vesicle solution and extensively washed with water. From the experimental point of view, it is worth emphasizing that the repeated dipping of the electrode in the various solutions did not wash out the lipid layer. In contrast with the loss of the layer observed when it is deposited on a planar surface (Brian and McConnell, 1984), the special geometry of the microporous template protects the structure when the tip of the electrode crosses the air/water interface.

Three questions must then be answered.

Do the unilamellar vesicles of DMPC adsorb and fuse as a monolayer onto the OTS surface?

It has already been demonstrated that such a monolayer fusion technique is effective on hydrophobic surfaces with various lipids, neutral or not (Brian and McConnell, 1984; Kalb et al., 1992; Torchut et al., 1994). The amounts of DMPC in the monolayer were determined here by radioac-

tive labeling. We found (Table 1) a DMPC stable surface concentration Γ_{DMPC} of 250 ± 50 pmol · cm^{-2} very close to the recent result of Nollert et al. (1995) (275 pmol cm^{-2} for a planar monolayer). This surface concentration is unaffected by the presence of the quinone. As the area occupied by a phospholipid molecule is about 60 $Å^2$ (Brian and McConnell, 1984), the value found for Γ_{DMPC} corresponds, as expected, to a single monolayer. In our case, the relatively high standard deviation in Γ_{DMPC} reflects the uncertainty on the internal surface area of the porous oxide structure rather than errors in the measurement of radioactivity.

Is the vesicle quinone/lipid ratio kept unchanged in the final supported layer?

Applying the spectrophotometric method described by Kröger (1978), it is easy to measure N_{UQ10}, the mole fraction of UQ_{10}, oxidized or reduced, in vesicle suspensions. However, the amount of quinone per unit surface area of bilayer (typically, 5 pmol·cm^{-2}) was so low that we chose to use aluminum oxide films, which are larger and thicker than our microporous electrodes, i.e., ~3 cm^2 of 50-μm-thick films of Anodisc membrane, giving an actual surface area of ~1500 cm^2 instead of 3.7 cm^2 for a typical porous oxide electrode. The surface concentrations of ubiquinone (Γ_{UQ10}) and DMPC (Γ_{DMPC}) were measured after common extraction from the thick films. Typical data are given in Table 1. Within experimental uncertainty, identical values were found for Γ_{DMPC} on thick films and on thin film-coated electrodes, a result confirming that the surface area of the thick oxide films was correctly evaluated. Then Γ_{UQ10} in the bilayers was deduced from the spectrophotometrical measurement of the surface concentration of UQ_{10} after extraction. Starting with three different concentrations of UQ_{10}, it appeared that Γ_{UQ10} remained unchanged, within experimental uncertainty, when going from the vesicles to the supported layers (Table 1). This means that during fusion, all of the molecules of each vesicle are spread out as a monolayer on the OTS layer. At the end of the fusion mechanism, UQ_{10} molecules are thus disposed between one OTS layer and one DMPC layer, as they were disposed before vesicle fusion between two DMPC layers. The concentration of isoprenic quinones in biological membranes is defined as a mole fraction taking into account the total amount of lipids in the two layers. Accordingly, the mole fraction of quinone in the asymmetrical supported bilayer is thus half the vesicle mole fraction. The quinone concentrations introduced here, in the supported bilayers, vary from ~1 to 3 mol % and are within the physiological range for isoprenic quinones (Hauska and Hurt, 1982).

The mechanism of pure phospolipid vesicle fusion proposed, on hydrophobic surfaces, by Kalb et al. (1992) could explain the incorporation of quinone into the supported asymmetrical bilayer. The proposed schematic pathway (see figure 6 in the paper by Kalb et al., 1992) could be easily adapted in such a manner that the hydrophobic UQ_{10} molecules would be permanently protected against the water by a lipid layer. From the energetic point of view, there is no reason to believe that the presence of UQ_{10} molecules may significantly reduce the strong hydrophobic interactions that are believed to provide the driving force for vesicle fusion.

Are the components laterally mobile in the layer?

With the help of a chronocoulometric method, it has already been demonstrated that the lateral mobilities of DMPC and UQ_{10} could be measured in microporous electrodes (Torchut et al., 1994). Using the same method, we found here a routine lateral diffusion coefficient of UQ_{10} similar to the previous measurements (~2 × 10^{-8} $cm^2 \cdot s^{-1}$ at 30°C) and to the value obtained by fluorescence recovery after photobleaching measurements (Rajarathnam et al., 1989). The fluidity of the supported lipid plus quinone layer, a decisive quality criterion for supported model membranes (Brian and McConnell, 1984), was thus established.

Two-dimensional electrochemistry of isoprenic quinones in the bilayer

Number of electrons involved in the redox process

Cyclic voltammetry was used to study the kinetics of electron tranfer between the electrode and the oxidized or re-

TABLE 1 Mass balances of UQ_{10} and DMPC before and after vesicle fusion on thin or thick oxide films

Vesicles before fusion		Supported layer (thin oxide film electrodes)				Supported layer (thick oxide films)			
UQ_{10} molar fraction (N_{UQ10})				Amount of UQ_{10}* from voltammetry				Amount of UQ_{10}# from absorbance	
Weighing (mol %)	Measured# (mol %)	Oxide area‖ (cm^2)	Γ_{DMPC}§ (pmol cm^{-2})	Γ_{UQ10} (pmol cm^{-2})	N_{UQ10} (mol %)	Oxide area‖ (cm^2)	Γ_{DMPC}§ (pmol cm^{-2})	Γ_{UQ10} (pmol cm^{-2})	N_{UQ10} (mol %)
0	0	3.7 ± 0.7	250 ± 50	0	0	(various)	250 ± 50	0	0
2.00	**1.91** ± 0.04	3.7 ± 0.7	230 ± 50	5.0 ± 1.0	**2.1** ± 0.4	2300 ± 400	210 ± 50	4.2 ± 0.8	**2.0** ± 0.4
4.00	**3.83** ± 0.06	3.7 ± 0.7	250 ± 50	8.9 ± 2.0	**3.5** ± 0.7	1700 ± 300	250 ± 50	10.0 ± 2.0	**3.8** ± 0.8
6.00	**5.83** ± 0.10	3.7 ± 0.7	240 ± 50	15.1 ± 3.0	**5.9** ± 1.2	1400 ± 300	250 ± 50	13.9 ± 2.5	**5.3** ± 1.1

The results were identical, within experimental uncertainty, when PQ_9 or $UQ_{10}H_2$ was incorporated into vesicles.
*From the integration of the voltammetric peaks scanned at 0.001 V s^{-1}, with 2 electrons per quinone.
#From the spectra in chloroform after extraction.
§From radioactive labeling.
‖Actual hydrophobic surface area of the microporous template.

duced quinone species located in the bilayer. According to the structure presented in Fig. 1, lateral diffusion of the quinones from the pores feeds the electrochemical reaction at the interface between the bilayer and the gold electrode, which mimics the redox site of integral proteins embedded in the bilayer. As in biological membranes, water molecules, protons, and possibly buffer components may be available for reaction with the quinone heads. It is worth emphasizing that a very satisfactory signal-to-noise ratio is obtained. It is provided by the high ratio of the supported bilayer area over the gold area. The unique porous geometry of the aluminum oxide template allows the precise determination of the bilayer quinone content, even at a level as low as 5 pmol · cm^{-2}.

At very low potential scan rate v, the time scale of the measurement is large enough to ensure that all of the active redox molecules can reach the electrode by lateral diffusion. For example, at $v = 0.001$ V s^{-1}, the cathodic and anodic currents always decrease back to the background current within less than 200 mV beyond the peak potential, as shown in Fig. 2. Then, at such a potential scan rate, the area under the peak gives the amount of electricity needed to reduce (or oxidize) all of the molecules of UQ_{10} or PQ_9 (or $UQ_{10}H_2$ or PQ_9H_2) included in the phospholipid layer (Laviron, 1980, 1984; Laviron et al., 1980). We found that the peak areas were pH independent in the studied range (4–13.2). Because the number of quinone molecules introduced in the phospholipid layer could be known independently as already described, the measurement of these areas enabled us to conclude that 2.0 ± 0.3 electrons per quinone species were involved in the electrochemical process. As can be seen in Table 1, the amount of UQ_{10} electrochemically determined, once the occurrence of a two-electron transfer is assumed, and the amount of UQ_{10} determined after solvent extraction were found to be identical within experimental uncertainty. Such a result provides further evidence of the mobility of all of the molecules of the quinone pool in this range of low mole fractions (1–3 mol%).

An alternative method was used to confirm the number of electrons electrochemically involved in the bilayer. KBH_4 is known to reduce UQ_n to UQ_nH_2 in vesicles at pH 7. The bielectronic reduction of UQ_{10} to $UQ_{10}H_2$ gives rise to a characteristic absorption band at 288 nm (Morrison et al., 1982). A microporous electrode, loaded with lipids and UQ_{10} at a mole fraction of ~2 mol%, was first scanned in the same conditions as in Fig. 2 (pH 7). The electrode was then submitted to KBH_4 reduction in another cell, which was also protected against oxygen. After rinsing, a new reduction scan starting at a potential $E = -100$ mV did not exhibit the UQ_{10} reduction peak. However, in the reverse scan an oxidation peak appeared with the expected coulombic area, thus demonstrating that both the electrochemical and chemical processes involved an overall two-electron transfer.

pH dependence of the quinone redox behavior

The cyclic voltammograms recorded at $v = 0.1$ V s^{-1} and at various pH are reproduced for UQ_{10} in Fig. 3. The initial potential E_i is positive enough to ensure that there is no appreciable current flowing at E_i. The potential is then scanned negatively until the observation of the cathodic

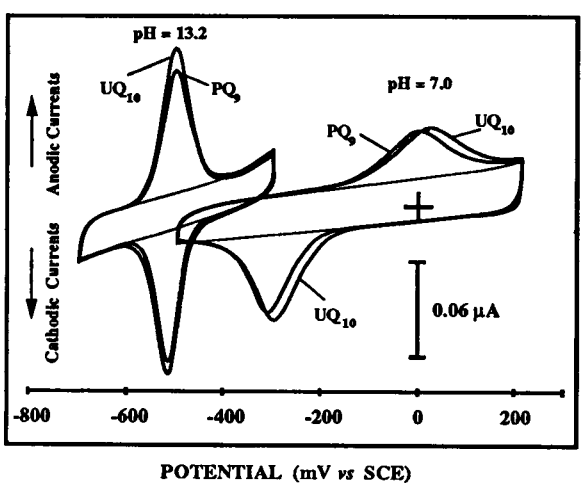

FIGURE 2 Cyclic voltammograms, at low scan rate, of UQ_{10} and PQ_9 solubilized in the supported bilayer structure. Scan rate: 0.001 V · s^{-1}. Background: NaOH 0.15 M or 0.01 M phosphate buffer. Temperature: 30°C. Background currents are represented by thin lines. The peak areas give mole fractions of 1.7 and 1.3 mol% for UQ_{10} and PQ_9, respectively.

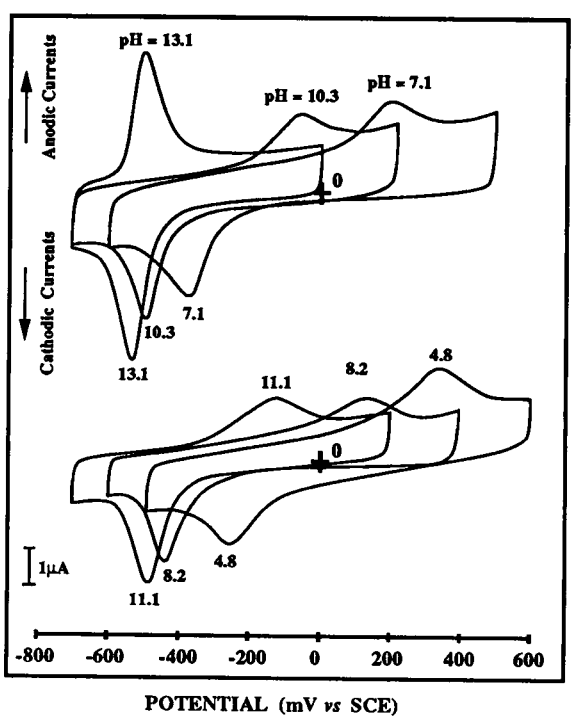

FIGURE 3 Effect of pH on the shape of the cyclic voltammograms of UQ_{10} in the supported bilayer structure. Scan rate: 0.1 V · s^{-1}. The crosses indicate zero potential and zero current for both series. Background currents were omitted for clarity. The surface concentration of UQ_{10} = 15.9 pmol · cm^{-2}, equivalent to a molar fraction of 3.0 mol %, was determined in a preliminary experiment at 0.001 V · s^{-1}.

peak (peak potential E_{pc}) corresponding to the electrochemical reduction of UQ_{10}. The reversal potential E_r is chosen so that $E_{pc} - E_r \geq 120$ mV. An anodic peak corresponding to the regeneration of UQ_{10} appears in the reverse scan at a peak potential E_{pa}.

Because a two-electron transfer takes place, the reduced form of UQ_{10} is either the fully protonated hydroquinone $UQ_{10}H_2$ or its monodeprotonated form $UQ_{10}H^-$. The related redox and acid-base reactions are

$$Q + 2e + 2H^+ \rightleftarrows QH_2 \qquad E^{o\prime}_{QH_2/Q} = E^{\circ}_{QH_2/Q,pH=0} - 60.2\,pH$$

$$Q + 2e + H^+ \rightleftarrows QH^- \qquad E^{o\prime}_{QH^-/Q} = E^{\circ}_{QH^-/Q,pH=0} - 30.1\,pH$$

$$QH_2 \rightleftarrows QH^- + H^+ \qquad K_{aQH_2} = (QH^-)(H^+)/(QH_2)$$

In the preceding equations, Q stands for the oxidized form of UQ_n or PQ_n and QH_2 for the reduced form UQ_nH_2 or PQ_nH_2. The redox potentials are expressed in millivolts versus the normal hydrogen electrode (NHE), and the temperature is 30°C.

At pH > 13, the electrochemical process exhibits a remarkable reversibility. When the thickness δ of the diffusion layer, calculated for semiinfinite linear diffusion toward the electrode, is much larger than the length l of the phospholipid layer (i.e., the length of the pores) as occurs at $v = 0.001$ V s^{-1}, all of the molecules are reduced within the time scale of the forward potential scan, and E_{pa} and E_{pc} are almost identical. For higher scan rates, the thickness of the diffusion layer being proportional to $v^{-1/2}$, δ may become much smaller than l, and the current becomes diffusion controlled and can be easily simulated (Nicholson and Shain, 1964; Nadjo and Savéant, 1973; Andrieux and Savéant, 1986). In our case, the simulation ascertains that such a condition is very well fulfilled at $v = 0.1$ V s^{-1}, with $D = 2 \times 10^{-8}$ cm^2 · s^{-1} and $l \geq 3$ μm. Particularly at pH > 13, $\Delta E_p = E_{pa} - E_{pc} = 30$ mV, as expected for a diffusion-controlled two-electron electrochemical process, in which the electron transfers are not rate determining (Andrieux and Savéant, 1986). For UQ_{10} the apparent redox standard potential $E^{\circ\prime}$ of the process at pH 13.1 is found to be $(E_{pa} + E_{pc})/2 = -515 \pm 5$ mV versus SCE or -277 ± 5 mV versus NHE at 30°C. For PQ_9, $E^{\circ\prime} = -282 \pm 5$ mV versus NHE at pH 13.2 and 30°C, i.e., the two quinones exhibit identical behaviors in the bilayer, and the following discussion applies to both molecules.

Below pH 13, the separation between the cathodic and anodic peaks exceeds 30 mV, as shown in Figs. 3 and 4. The pH decrease causes a decrease in the reversibility of the electrochemical process, and the higher the v, the greater the peak separation (not shown). The most likely explanation is that the cyclic voltammogram observed at pH 13 corresponds to the QH^-/Q redox system, in which the electron transfers and the proton transfer proceed at equilibrium. Full reversibility is lost as a result of the protonation of QH^- into QH_2. From the plot reproduced in Fig. 4, it can be deduced that pK_{aQH2} is 12.5 ± 0.2, because at pH < pK_{aQH2}, the peak separation ΔE_p is appreciably greater than 30 mV, whereas at pH > pK_{aQH2}, ΔE_p is 30 mV. The reduction of

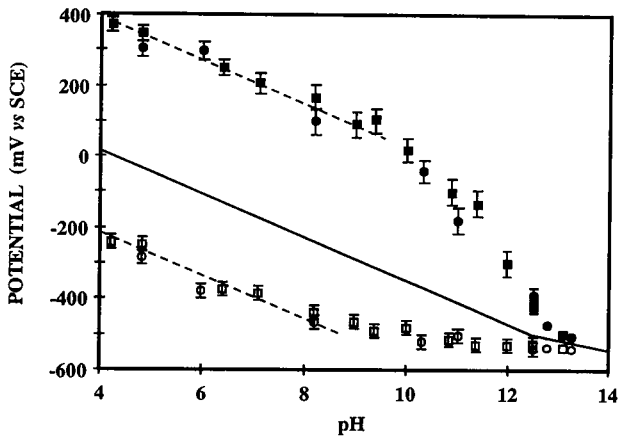

FIGURE 4 pH dependence of the anodic (●, ■) and cathodic (○, □) peak potentials at a scan rate of 0.1 V · s^{-1}. Different porous electrodes loaded either with UQ_{10}/DMPC (□, ■) or PQ_9/DMPC (○, ●). The continuous line gives the pH-potential variation according to 255 − 60.2 pH (mV versus SCE) for pH < 12.5 and −121 − 30.1 pH (mV *vs.* SCE) for pH > 12.5. Temperature: 30°C. The slopes of the dotted lines are 60.2 mV/pH.

Q to Q^{2-} must be disregarded, because it would imply the occurrence of two successive one-electron transfers without the contribution of any proton transfer. In that case two successive cathodic peaks separated by ~500 mV, each one being monoelectronic, should be recorded (Marcus and Hawley, 1971; Chambers, 1974).

In the 9–12 pH region, E_{pc} is roughly pH independent. This results from the mutual cancellation of two effects of opposite directions. Because of consecutive protonation of QH^-, E_{pc} should shift positively with decreasing pH (Nadjo and Savéant, 1973; Andrieux and Savéant, 1986). Simultaneously, the initial heterogeneous electron transfer becomes more and more rate controlling, because the proton transfers become faster and faster. Thus E_{pc} should shift negatively with decreasing pH. On the other hand, for the anodic peak a rather steep positive shift of E_{pa} is observed in the same pH region when the pH decreases (Fig. 4). Then there is a contribution of two effects in the same direction. The deprotonation of QH_2 must precede the electrochemical reaction, and the initial heterogeneous electron transfer becomes more and more rate controlling. Each phenomenon should bring about a positive shift of E_{pa} and a broadening of the peak, with a concomitant decrease in its height (Nicholson and Shain, 1964; Nadjo and Savéant, 1973; Andrieux and Savéant, 1986).

Below pH 9, both the cathodic and anodic currents are controlled by the rates of initial heterogeneous electron transfers and diffusion and can again be easily simulated. As can be seen in Fig. 4, the rates of the cathodic and anodic heterogeneous electron transfers exhibit a pH dependence of ~60 mV/pH, similar to what was observed when UQ_{10} was adsorbed onto a mercury electrode (Gordillo and Schiffrin, 1994).

Potential-pH plots, more or less similar to the one reproduced in Fig. 4, have already been reported in several

instances, the isoprenic quinones being adsorbed onto various types of electrode surfaces (Gordillo and Schiffrin, 1994; Sanchez et al., 1995). In the present paper we wish to emphasize that all thermodynamic deductions must be anchored only in the experimentally observed reversible behavior of the QH^-/Q redox couples at pH > 13 and in the fact that the departure from reversibility is caused by the protonation of QH^-, the pK_{aQH2} being known.

The following deductions can be drawn from the results and data presented above.

Starting with

$$E^{\circ\prime}_{QH^-/Q,pH\ 13.1} = -277 \pm 5\ \text{mV versus NHE}$$

and

$$pK_{aQH_2} = 12.5 \pm 0.2$$

we find

$$E^{\circ\prime}_{QH^-/Q,pH=0} = E^{\circ\prime}_{QH^-/Q,pH\ 13.1} + 30.1 \times 13.1 = 114 \pm 5\ \text{mV}$$

and

$$E^{\circ\prime}_{QH^-/Q,pH\ 7} = E^{\circ\prime}_{QH^-/Q,pH=0} - 30.1 \times 7$$
$$= -94 \pm 5\ \text{mV vs. NHE}$$

Taking into account that, at $pH = pK_{aQH2} = 12.5 \pm 0.2$:

$$E^{\circ\prime}_{QH_2/Q,pH\ 12.5} = E^{\circ\prime}_{QH^-/Q,pH\ 12.5} = -262 \pm 10\ \text{mV}$$

then

$$E^{\circ\prime}_{QH_2/Q,pH\ 0} = E^{\circ\prime}_{QH_2/Q,pH\ 12.5} + 60.2 \times 12.5$$
$$= 491 \pm 10\ \text{mV}$$

and

$$E^{\circ\prime}_{QH_2/Q,pH\ 7} = 72 \pm 10\ \text{mV versus NHE}$$

The values thus calculated for the formal potentials at pH 7 (Table 2) are in agreement with those determined previously in the presence of 80% ethanol (Rich, 1984). There is also quite satisfactory agreement with those determined when UQ_{10} was incorporated into a self-assembled phospholipid monolayer (Moncelli et al., 1996) or was adsorbed directly at a mercury electrode (Gordillo and Schiffrin, 1994). In the latter case, pK_{aQH2} was also found to be rather high (i.e., 12). This suggests that it is reasonable to assume that the local pH in the DMPC layer is identical with that of the surrounding solution, as we did implicitly when we stated above that $pK_{aQH2} = 12.5 \pm 0.2$ in the DMPC layer. Further confirmation was obtained as follows. The water solubility of ubiquinone UQ_2 was high enough to allow us direct voltammetric measurements with a bare gold electrode introduced into the UQ_2 solution. The cyclic voltammetric behavior showed that both UQ_2 and UQ_2H_2 adsorb strongly at the gold/water interface, whereas UQ_2H^- desorbs rapidly. This provided us with a means of determining pK_{aUQ2H2}. We found that $pK_{aUQ2H2} = 12.4 \pm 0.2$. Because there is no reason to assume that $pK_{aUQ10H2}$ and pK_{aUQ2H2} differ appreciably, it shows that the thermodynamic data determined here in the supported bilayer environment are not affected by the interference of a local pH effect.

Reactivity of the semiquinone species

The thermodynamics of the semiquinone formation and reactivity can also be discussed. The semiquinone $Q^{\bullet -}$ may also exist in its protonated form $QH^\bullet$. The electron and proton transfers involving the semiquinone species in the pH range of physiological interest are

$Q + e \rightleftarrows Q^{\bullet -}$	$E^\circ_{Q^{\bullet -}/Q}$
$Q^{\bullet -} + e \rightleftarrows Q^{2-}$	$E^\circ_{Q^{2-}/Q^{\bullet -}}$
$QH^\bullet \rightleftarrows Q^{\bullet -} + H^+$	$pK_{aQH^\bullet}$
$QH^\bullet + e \rightleftarrows QH^-$	$E^\circ_{QH^-/QH^\bullet}$
$QH^\bullet + e + H^+ \rightleftarrows QH_2$	$E^{\circ\prime}_{QH_2/QH^\bullet} = E^\circ_{QH_2/QH^\bullet,pH0} - 60.2\ pH$

TABLE 2 Thermodynamic constants of isoprenic quinones at pH 7

	UQ_{10}			PQ_9	
Formal potential or pK	In ethanol/water solutions	Adsorbed on Hg*	In supported# bilayer	In ethanol/water solutions	In supported# bilayer
$E^{\circ\prime}_{QH_2/Q}$	70§	104	72 ± 10	110§	72 ± 10
$E^{\circ\prime}_{QH^-/Q}$	−54§	−57	−94 ± 10	−3§	−94 ± 10
$E^\circ_{Q^{-\bullet}/Q}$	−230 ± 20‖	—	(−230 ± 20)‖	−130 ± 20‖	(−130 ± 20)‖
$E^\circ_{QH^\bullet/QH^-}$	190§	227	170 ± 30¶	240§	80 ± 30¶
pK_{aQH_2}	11.2§	12.0	12.5 ± 0.3	10.8§	12.5 ± 0.5
$pK_{aQH^\bullet}$	4.9‖	5.5	(4.9)‖	4.7‖	(4.7)‖

Potentials in mV versus ENH. T = 25 or 30°C.
*From Gordillo and Schiffrin (1994), at 25°C.
#This work at 30°C.
§From Rich (1984), evaluated at 25°C from model quinone behavior in protic solvents.
‖From Swallow (1982), evaluated at 25°C from model quinone behavior in protic solvents.
¶Calculated from $E^\circ_{QH^\bullet/QH} = -[RT/F \ln(K_{aQH^\bullet}) + E^\circ_{Q^{-\bullet}/Q} + 2E^\circ_{QH^-/Q}]$.

The disproportionation the semiquinone cannot proceed through the reaction of two $Q^{\bullet -}$ because, as already mentioned, $E^{\circ}_{Q^{2-}/Q^{\bullet -}}$ is much more negative than $E^{\circ}_{Q^{\bullet -}/Q}$ (Marcus and Hawley, 1971; Chambers, 1974). Estimations of both $E^{\circ}_{Q^{\bullet -}/Q} = -230 \pm 20$ mV versus NHE and $pK_{aQH^{\bullet}} = 4.9$ for UQ_{10} and $E^{\circ}_{Q^{\bullet -}/Q} = -130 \pm 20$ mV versus NHE and $pK_{aQH^{\bullet}} = 4.7$ for PQ_9 can be found in the literature (Swallow, 1982).

Then

$$E^{\circ}_{QH^{-}/QH^{\bullet}} = -E^{\circ}_{Q^{\bullet -}/Q} + 2E^{\circ}_{QH^{-}/Q,pH=0} - 60.2\ pK_{aQH^{\bullet}}$$

and

$$E^{\circ\prime}_{QH_2/QH^{\bullet},pH7} = E^{\circ}_{QH^{-}/QH^{\bullet}} + 60.2(pK_{aQH_2} - 7)$$

For UQ_{10} that gives

$$E^{\circ}_{QH^{-}/QH^{\bullet}} = 160 \pm 30\ \text{mV}$$

and

$$E^{\circ\prime}_{QH^2/QH^{\bullet},pH7} = 490 \pm 40\ \text{mV versus NHE}$$

and for PQ_9:

$$E^{\circ}_{QH^{-}/QH^{\bullet}} = 80 \pm 30\ \text{mV}$$

and

$$E^{\circ\prime}_{QH_2/QH^{\bullet},pH7} = 410 \pm 40\ \text{mV versus NHE}$$

The potentials of the redox systems involving the semiquinone species are such that the disproportionation of the semiquinone must proceed through the reaction between $QH^{\bullet}$ and $Q^{\bullet -}$, the driving force of which is very strong, inasmuch as it exceeds 200 mV. This means that the bimolecular disproportionation of the semiquinone is complete at equilibrium. Its rate is controlled either by the diffusion of the semiquinone species within the supported bilayer, with the acid-base $QH^{\bullet}/Q^{\bullet -}$ transformation acting as a preequilibrium, or by the activation needed, after encounter, to bring the semiquinone species into conformations allowing the occurrence of an efficient electron transfer between the two redox centers. Such a conclusion still holds, at least for UQ_{10}, even if the inaccuracies of the estimations of $E^{\circ}_{Q^{\bullet -}/Q}$ and $pK_{aQH^{\bullet}}$ are as large as 60 mV and one pK_a unit, respectively.

CONCLUSION

The methodology presented here makes it possible to control the redox state of the mobile quinone pool introduced in the hydrophobic interlayer of an artificial bilayer structure. A self-assembly strategy is used for the step-by-step construction of a supported bilayer at the interface of a modified electrode. Long-chain alkylated silane molecules are grafted inside the pores of an aluminum oxide template to build the first hydrophobic layer. Then the lipid layer results from the occurrence of a vesicle fusion mechanism, which introduces simultaneously the long-chain isoprenic quinone molecules at physiological concentration. The achievement of this second step is quantitatively characterized. From the electrochemical point of view, the amount of redox molecules being rather low, a key point is the convenient signal-to-noise ratio obtained with the help of the microporous structure.

For the two types of long-chain isoprenic quinones that were examined in the present study, the values found in the bilayer for the thermodynamic characteristics differ slightly from those used currently in the biochemical literature. The first aspect is that the redox behaviors of ubiquinones and plastoquinones appear, from our measurement, quite identical. This is surprising, because the biochemical literature admits in general that the plastoquinone potentials are slightly higher (~40 mV for $E^{\circ\prime}_{QH_2/Q}$, for example). The second aspect is that, as a result, the discrepancies with the literature are larger for plastoquinone (see Table 2). Then it must be underlined that, in the case of plastoquinone, the thermodynamic characteristics given in the literature were estimated mainly by analogy with a rough model molecule, i.e., trimethyl-*p*-benzoquinone, solubilized in ethanol/water solutions. As the measurements were performed here in similar conditions for both UQ_{10} and PQ_9, and as the physicochemical environment of the quinone molecules was then closer to the one existing in a biological membrane, our results show that the relevant characteristics of the quinol and quinone species of UQ_{10} and PQ_9 do not differ significantly. For the semiquinones species, the values of $E^{\circ}_{Q^{\bullet -}/Q}$ and $pK_{aQH^{\bullet}}$ cannot be determined by means of the electrochemical approach used in the present work. However, it seems reasonable to assume that the disproportionation of the semiquinone is complete at equilibrium.

REFERENCES

Andrieux, C. P., and J-M. Savéant. 1986. Electrochemical reactions. *In* Investigation of Rates and Mechanisms of Reactions. C. P. Bernasconi, editor. Techniques of Chemistry, Vol. 6, Part 2. Wiley-Interscience, New York. 305–390.

Brian, A. A., and H. M. McConnell. 1984. Allogeneic stimulation of cytotoxic T cells by supported planar membranes. *Proc. Natl. Acad. Sci. USA.* 81:6159–6163.

Cauquis, G., and G. Marbach, G. 1972. Influence de divers donneurs de protons sur les propriétés oxydoréductrices de l'ubiquinone 6 en milieu organique. *Biochim. Biophys. Acta.* 283:239–246.

Chambers, J. Q. 1974. Electrochemistry of quinones. *In* The Chemistry of the Quinonoid Coumpounds. S. Patai, editor. John Wiley and Sons, New York. 737–791.

Crane, F. L., and R. Barr. 1985. Chemical structure and properties of coenzyme Q and related compounds. *In* Coenzyme Q. G. Lenaz, editor. Wiley and Sons, Chichester, England. 1–37.

Gennis, R. B. 1989. *In* Biomembranes, Molecular Structure and Function. Springer Verlag, New York. 166–197.

Gordillo, G. J., and J. Schiffrin. 1994. Redox properties of ubiquinone adsorbed on a mercury electrode. *J. Chem. Soc. Faraday Trans.* 90: 1913–1922.

Hauska, G., and E. Hurt. 1982. Pool function behavior and mobility of isoprenoid quinones. *In* Function of Quinones in Energy Conserving Systems. P. L. Trumpower, editor. Academic Press, New York. 87–110.

Kalb, E., S. Frey, and L. K. Tamm. 1992. Formation of supported planar bilayers by fusion of vesicles to supported phospholipid monolayers. *Biochim. Biophys. Acta.* 1103:307–316.

Kröger, A. 1978. Determination of contents and redox states of ubiquinone and menaquinone. *In* Methods in Enzymology, Vol. 53. S. Fleisher and L. Packer, editors. Academic Press, New York. 579–591.

Ksenzhek, O. S., S. A. Petrova, and M. V. Kolodyazhny. 1982. Redox properties of ubiquinones in aqueous solutions. *Bioelectrochem. Bioenerg.* 9:167–174.

Land, E. J., and A. J. Swallow. 1970. One electron reactions in biological systems as studied by pulse radiolysis. *J. Biol. Chem.* 245:1890–1894.

Laviron, E. 1980. A multilayer model for the study of space distributed redox modified electrodes. Part I. Description and discussion of the model. *J. Electroanal. Chem.* 112:1–9.

Laviron, E. 1984. Electrochemical reactions with protonations at equilibrium. Part X. The kinetics of the *p*-benzoquinone/hydroquinone couple on a platinum electrode. *J. Electroanal. Chem.* 164:213–227.

Laviron, E., L. Roullier, and C. Degrand. 1980. A multilayer model for the study of space distributed redox modified electrodes. Part II. Theory and application of linear potential sweep voltammetry for a simple reaction. *J. Electroanal. Chem.* 112:11–23.

Marcus, M. F., and M. D. Hawley. 1971. Electrochemical studies of the redox behavior of ubiquinone. *Biochim. Biophys. Acta.* 226:234–238.

Meunier-Prest, R., and E. Laviron. 1992. Electrochemical reactions with protonations at equilibrium. Part XV. The $2e^-$, $2H^+$ bi-cubic scheme. *J. Electroanal. Chem.* 328:33–46.

Miller, C. J., and M. Majda. 1986. Microporous aluminium oxide films at electrodes. 3. Lateral electron transport in self-assembled monolayers of *N*-methyl-*N'*-octadecyl-4,4'-bipyridinium chloride. *J. Am. Chem. Soc.* 108:3118–3120.

Moncelli, M. R., L. Becucci, A. Nelson, and R. Guidelli. 1996. Electrochemical modeling of electron and proton transfer to ubiquinone-10 in a self-assembled phospholipid monolayer. *Biophys. J.* 70:2716–2726.

Morrison, L. E., J. E. Schelhorn, T. M. Cotton, C. L. Bering, and P. A. Loach. 1982. Electrochemical and spectral properties of ubiquinone and synthetic analogs. *In* Function of Quinones in Energy Conserving Systems. P. L. Trumpower, editor. Academic Press, New York. 35–68.

Nadjo, L., and J-M. Savéant. 1973. Linear sweep voltammetry: kinetic control by charge transfer and/or secondary chemical reactions. I. Formal kinetics. *J. Electroanal. Chem.* 48:113–145.

Nicholson, R. S., and I. Shain. 1964. Theory of stationary electrode polarography. Single scan and cyclic methods applied to reversible, irreversible, and kinetic systems. *Anal. Chem.* 36:706–723.

Nollert, P., H. Kiefer, and F. Jahning. 1995. Lipid vesicle adsorption versus formation of planar bilayers on solid surfaces. *Biophys. J.* 69: 1447–1455.

Okamura, M., and G. Feher. 1992. Proton transfer in reaction centers from photosynthetic bacteria. *Annu. Rev. Biochem.* 61:861–896.

Parpaleix, T., J. M. Laval, M. Majda, and C. Bourdillon. 1992. Potentiometric and voltammetric investigations of H_2/H^+ catalysis by periplasmic hydrogenase from *D. gigas* immobilized at the electrode surface in an amphiphilic bilayer assembly. *Anal. Chem.* 64:641–646.

Pileni, M. P., A. M. Braun, and M. Gratzel. 1980. Light driven redox processes in functional micellar units. III. Zn-tetraphenylporphyrin sensitized reactions in methyl viologen surfactant assemblies. *Photochem. Photobiol.* 31:423–427.

Prince, R. C., P. L. Dutton, and J. M. Bruce. 1983. Electrochemistry of ubiquinones, menaquinones and plastoquinones in aprotic solvents. *FEBS Lett.* 160:273–276.

Prince, R. C., P. Lloyd-Williams, J. M. Bruce, and P. L. Dutton. 1986. Voltammetric measurement of quinones. *In* Methods in Enzymology. S. Fleisher and B. Fleisher, editors. Academic Press, New York. 109–119.

Rajarathnam, K., J. Hochman, M. Schindler, and S. Fergusson-Miller. 1989. Synthesis, location, and lateral mobility of fluorescently labeled ubiquinone 10 in mitochondrial and artificial membranes. *Biochemistry.* 28:3168–3176.

Rich, P. R. 1984. Electron and proton transfers through quinones and cytochrome bc complexes. *Biochim. Biophys. Acta.* 768:53–79.

Sanchez, S., A. Arratia, R. Cordova, H. Gomez, and R. Schrebler. 1995. Electron transport in biological processes. Electrochemical behavior of Q_{10} immersed in a phopholipidic matrix added on a pyrilitic graphite electrode. *Bioelectrochem. Bioenerg.* 36:67–71.

Schrebler, R. S., A. Arratia, S. Sanchez, M. Haun, and N. Duran. 1990. Electron transport in biological processes. Electrochemical behavior of ubiquinone Q_{10} adsorbed on a pyrolitic graphite electrode. *Bioelectrochem. Bioenerg.* 23:81–91.

Swallow, A. J. 1982. Physical chemistry of quinones. *In* Function of Quinones in Energy Conserving Systems. P. L. Trumpower, editor. Academic Press, New York. 59–72.

Takehara, K., and Y. Ide. 1991. Electrochemical behavior of the ubiquinone-Q_{10} film coated onto a glassy carbon electrode by the spinner method. *Bioelectrochem. Bioenerg.* 26:297–305.

Takehara, K., H. Takemura, Y. Ide, and S. Okayama. 1991. Electrochemical behavior of ubiquinone and vitamin K incorporated into *n*-alkanethiol molecular assemblies on a gold electrode. *J. Electroanal. Chem.* 308:345–350.

Torchut, E., J-M. Laval, C. Bourdillon, and M. Majda. 1994. Electrochemical measurements of the lateral diffusion of electroactive amphiphiles in supported phospholipid monolayers. *Biophys. J.* 66:753–762.